Proceedings of the 17th World Congress
The International Federation of Automatic Control
Seoul, Korea, July 6-11, 2008

Output feedback control: a robust solution based on second order sliding mode

F. Plestan [*], **E. Moulay** [*], **A. Glumineau** [*], **T. Cheviron** [*,**]

[*] *IRCCyN, CNRS-Ecole Centrale de Nantes, 1 Rue de la Noë, 44312 Nantes Cedex 3, France, Franck.Plestan@irccyn.ec-nantes.fr*
[**] *LRBA-DGA, Forêt de Vernon, 27200 Vernon, France*

Abstract: This paper proposes a new second order sliding mode output feedback controller. In the continuous case for which sampling frequency is supposed infinite, this controller uses only the output information and ensures desired trajectory tracking in a finite time in spite of uncertainties and perturbations. Moreover, in case of finite sampling frequency, it is shown that the controller needs also the sign of output time derivative to ensure the finite time convergence to an origin neighborhood.

Keywords: Second order sliding mode, output feedback, robustness.

1. INTRODUCTION

High order sliding mode control is a nonlinear control strategy, robust with respect to uncertainties and perturbation. Several algorithms have been published, more or less usable on practical applications (Levant [2001], Bartolini et al., [2000], Laghrouche et al., [2007], Plestan et al., [2008]). Since few years, applications to experimental set-up have proved the feasibility and applicability of these approaches for robots (high-order sliding mode observers in (Lebastard et al., [2006], Lebastard et al., [2006a]), electrical machines (Plestan et al., [2008]), pneumatic actuators (Laghrouche et al., [2006]), (Girin et al., [2007]). However, a lack of higher order sliding mode control is the use of high order time derivatives of sliding variables; by a practical point-of-view, it can decrease the interest of such controllers, due to the bad effect of measurement noise on the control. In order to remove this lack, a mean is to consider output feedback. The objective is then to propose output feedback control which ensures both robustness and accuracy by minimizing the noise effect. Two kinds of approaches are possible: the first one consists in designing state observer coupled to a controller: it is necessary to verify the stability of the observer-based controlled system which is in main cases a hard task. In the case of high order sliding mode, it has been done in (Levant [2003]) but this solution suffers of a lack of constructibility.
Very few results are available on second order sliding mode static output feedback. In (Khan et al., [2003]), a second order sliding mode output feedback controller is proposed: its main drawback is the absence of a formal proof of the closed-loop system stability. This current paper proposes a constructive method for the design of an output feedback controller. It ensures the convergence in a finite time to the origin of the theoretical system and to a neighborhood of the origin of the real system.
The paper is organized as follows. Section 2 states the problem of high order sliding mode output feedback controller. Section 3 displays the design of the output feedback controller by detailing both bases of infinite (ideal) and finite sampling frequency. Section 4 applies the controller for speed control of a series DC motor.

2. PROBLEM STATEMENT

Consider a single-input nonlinear system

$$\begin{array}{l} \dot{x} = f(x) + g(x)u \\ y = h(x) \end{array} \quad (1)$$

with $x \in \mathbb{R}^n$ the state variable, $u \in \mathbb{R}$ the input, and $y \in \mathbb{R}$ a smooth output function. Let $s(x,t)$ denote the sliding variable defined as

$$s(x,t) = h(x) - h_d(t)$$

$h_d(t)$ being the smooth desired trajectory. f and g are smooth uncertain functions. Assume that

H1. The relative degree of (1) with respect to s is constant and equal to 2, and the associated zero dynamics are stable. Only the sliding variable s is measured. ■

The control objective is to fulfill the constraint $s(x,t) = 0$ in finite time and to keep it exactly by discontinuous output feedback control. Let us recall the definition of second order sliding mode given in Levant [2001]

Definition 1. Consider the nonlinear system (1), and let the system be closed by some possibly-dynamical discontinuous feedback. Then, provided that s and $\dot{s}$ are continuous functions, and the set

$$\mathbf{S} = \{x \mid s(x,t) = \dot{s}(x,t) = 0\},$$

called "second order sliding set", is non-empty and is locally an integral set in the Filippov sense (see Filippov [1988]), the motion on $\mathbf{S}$ is called *second order sliding mode* with respect to the sliding variable s.

The second order sliding mode output feedback control problem allows the finite time stabilization to zero of the sliding variable s and its first time derivatives by defining a suitable control function. The output s fulfills

$$\ddot{s} = \bar{a}(x) + b(x)u(s) - \dot{h}_d(t) := a(x,t) + b(x)u(s) \quad (2)$$

Assume that

H2. The solutions are understood in the Filippov sense (see Filippov [1988]), and the system trajectories are supposed to be infinitely extendible in time for any bounded Lebesgue measurable input. ■

H3. Functions $a(x,t)$ and $b(x)$ are bounded uncertain functions and $b(x)$ is strictly positive. Thus, there exists positive constants $b_m > 0$, $b_M > 0$ and $a_M \geq 0$ such that $0 < b_m < b(x) < b_M$ and

$$|a(x,t)| \leq a_M$$

for $x \in \mathbf{X} \subset I\!R^n$, $\mathbf{X}$ being a bounded open subset of $I\!R^n$ within which the boundedness of the system dynamics is ensured, and $t > 0$. ■

Then, by setting $z_1 = s$ and $z_2 = \dot{s}$, the second order sliding mode output feedback control of (1) with respect to the sliding variable s is equivalent to the finite time stabilization of the system

$$\dot{z}_1 = z_2, \quad \dot{z}_2 = a(\cdot) + b(\cdot) \cdot u(z_1) \tag{3}$$

under Assumptions H1-H3.

3. A FINITE TIME SECOND ORDER SLIDING MODE OUTPUT FEEDBACK CONTROLLER

In this section, solutions of output feedback controllers for linear systems and time-varying ones are proposed. These control laws will be used in order to define sliding surface and switching variables in the next section.

3.1 Preliminaries

From (3), consider the following double integrator without uncertainties

$$\dot{z}_1 = z_2, \quad \dot{z}_2 = u \tag{4}$$

where the control input u is a discontinuous output feedback reading as

$$u(z_1) = -K \text{ sign}(z_1)$$

with $K > 0$. As $\ddot{z}_1 = -K \text{ sign}(z_1)$, one gets

$$\begin{aligned} z_1(t) &= -K \text{ sign}(z_1) \frac{t^2}{2} + z_{2,0} t + z_{1,0} \\ z_2(t) &= -K \text{ sign}(z_1)\, t + z_{2,0} \end{aligned} \tag{5}$$

with $z_{1,0} := z_1(0)$ and $z_{2,0} := z_2(0)$. The equation of the phase portrait reads as

$$z_2^2 + 2K|z_1| = z_{2,0}^2 + 2K \text{sign}(z_1)\, z_{1,0}. \tag{6}$$

This equation leads to two branches of parabola $\mathcal{P}_K^+$ and $\mathcal{P}_K^-$, with horizontal z_1-axis of symmetry in the half-planes $z_1 > 0$ and $z_1 < 0$ (see Figure 1 for different values of K). The vertices which are the intersection points between the branches of parabola and the z_1-axis are given by (see Figure 1)

$$V = \left(\frac{z_{2,0}^2}{2K \text{ sign}(z_1)} + z_{1,0}, 0 \right). \tag{7}$$

The intersection points I between the branches of parabola and the z_2-axis are given by

$$\begin{aligned} I^+ &= \left(0, \sqrt{z_{2,0}^2 + 2K \text{ sign}(z_1)\, z_{1,0}}\right) \\ I^- &= \left(0, -\sqrt{z_{2,0}^2 + 2K \text{ sign}(z_1)\, z_{1,0}}\right). \end{aligned} \tag{8}$$

Note that I^+ and I^- are symmetric with respect to the horizontal z_1-axis. Without loss of generality, suppose

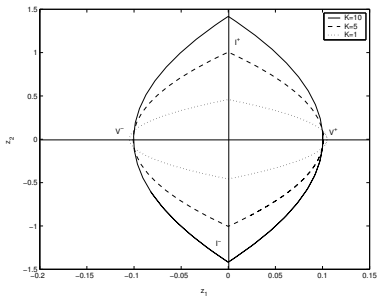

Fig. 1. Phase portrait of system (4) for several values of K.

that system (4) starts from initial values $z_1^0 > 0$, $z_2^0 > 0$. System (4) evolves on a branch of parabola $\mathcal{P}_K^+$ with vertex

$$V^+ = \left(\frac{z_{2,0}^2}{2K} + z_{1,0}, 0 \right). \tag{9}$$

From (5), it is obvious that, after a finite amount of time, system (4) reaches the vertical z_2-axis at the point I^-. Then, control input switches and system (4) is initialized at I^- by new values given by

$$(\overline{z_{1,0}}, \overline{z_{2,0}}) = \left(0, -\sqrt{z_{2,0}^2 + 2K\ z_{1,0}}\right).$$

It leads to a new branch of parabola $\mathcal{P}_K^-$ with a new vertex

$$\begin{aligned} V^- &= \left(\frac{\overline{z_{2,0}}^2}{2K \text{ sign}(z_1)} + \overline{z_{1,0}}, 0 \right) \\ &= \left(\frac{z_{2,0}^2 + 2K\ z_{1,0}}{-2K}, 0 \right) \\ &= \left(\frac{-z_{2,0}^2}{2K} - z_{1,0}, 0 \right). \end{aligned} \tag{10}$$

$\mathcal{P}_K^-$ is symmetric to $\mathcal{P}_K^+$ with respect to the z_2-axis. By the same way, it can be shown that, after a finite amount of time, system (4) reaches point I^+ and slides on $\mathcal{P}_K^+$. Finally, system (4) evolves on the two branches of parabola $\mathcal{P}_K^+$ and $\mathcal{P}_K^-$ and $\mathcal{P}_K^- \cup \mathcal{P}_K^+$ is symmetric with respect to the z_1-axis and the z_2-axis. Note also that initial point $\left(z_1^0, z_2^0\right)$ belongs to the curve $\mathcal{P}_K^-$.

Theorem 1. Under initial conditions $(z_{1,0}, z_{2,0})$, system (4) controlled by

$$u(z_1) = -K \text{ sign}(z_1), \qquad K > 0$$

is practically stable and evolves on two branches of parabola $\mathcal{P}_K^- \cup \mathcal{P}_K^+$ whose equations are given by (6) and vertices V by (7). ■

3.2 Robustness analysis

In order to evaluate the robustness of previous output feedback control class, consider system (3) with AssumptionsH1-H3 fulfilled and

$$u(z_1) = -K \text{ sign}(z_1).$$

From the previous result, it yields that system (3) is practically stable if for all $t \geq 0$,

$$\begin{aligned} a(\cdot) - b(\cdot)\ K < 0, &\qquad z_1 > 0 \\ a(\cdot) + b(\cdot)\ K > 0, &\qquad z_1 < 0. \end{aligned}$$

This latter condition is fulfilled if (for $t \geq 0$)

$$K > \frac{|a(\cdot)|}{b(\cdot)},\ t \geq 0 \qquad \Rightarrow \qquad K > \frac{a_M}{b_m}$$

Theorem 2. Under initial conditions $(z_{1,0}, z_{2,0})$ and assumptions H1-H3, system (3) controlled by

$$u \ = \ -K \ \text{sign}(z_1)$$

with $K > \dfrac{a_M}{b_m}$, is practically stable and evolves on

$$\mathcal{P} = \bigcup_{\alpha_m \leq \alpha \leq \alpha_M} \mathcal{P}_\alpha^- \cup \bigcup_{\beta_m \leq \beta \leq \beta_M} \mathcal{P}_\beta^+.$$

where $\alpha_m = -a_M - b_M K$, $\alpha_M = a_M - b_m K$, $\beta_m = -a_M + b_m K$ and $\beta_M = a_M + b_M K$. ■

The second part of Theorem 2 is due to the fact that, on $\mathcal{P}^-$ for $z_1 < 0$, we have

$$-a_M - b_M K < a\,(t) - b\,(t)\ K < a_M - b_m K$$

and on $\mathcal{P}^+$ for $z_1 > 0$, we have

$$-a_M + b_m K < a\,(t) + b\,(t)\ K < a_M + b_M K.$$

Remark 1. In the case where a and b are constant ($b \neq 0$), z_1-dynamics reads as

$$\ddot{z}_1 = a - b\ K\ \text{sign}\,(z_1)$$

It yields

$$\begin{array}{ll} \ddot{z}_1 \ = \ a - b\ K, & z_1 > 0 \\ \ddot{z}_1 \ = \ a + b\ K, & z_1 < 0 \end{array} \tag{11}$$

The fact that the system is no more symmetric in the half-planes $z_1 > 0$ and $z_1 < 0$, implies that $\mathcal{P}_K^+$ and $\mathcal{P}_K^-$ are no more symmetric with respect to the z_2-axis. The vertices are now defined by

$$V^+ = \left(\frac{z_{2,0}^2}{2\,(a - bK)} + z_{1,0}, 0 \right),$$

$$V^- = \left(\frac{z_{2,0}^2}{-2\,(a + bK)} + z_{1,0}, 0 \right)$$

and are not symmetric with respect to the z_2-axis (Figure 2).

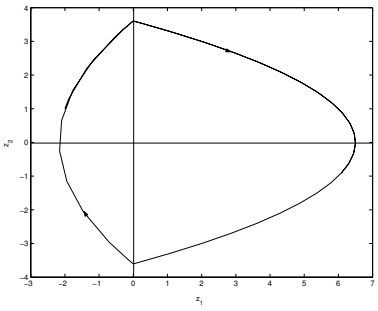

Fig. 2. Phase portrait of system (3) for $a = 1$, $b = 2$ and $K = 1$.

3.3 Extension in case of finite sample frequency

Suppose now that system (4) is viewed under a practical point-of-view, *i.e.* the sample frequency is finite inducing that the "sign" function does not switch instantaneously. Due to the finite sample time T_e, control input usually does not switch *exactly* on the z_2-axis, but with a delay bounded by the sample time value. From this latter remark, discontinuous control input of system (3) can be applied with a bounded delay $d(t)$, such that $0 \leq d(t) < T_e$: it yields that, under the finite sample frequency hypothesis, system (3) behavior is equivalent to behavior of

$$\begin{array}{l} \dot{z}_1\,(t) \ = \ z_2\,(t) \\ \dot{z}_2\,(t) \ = \ a\,(\cdot) - b\,(\cdot)\ K\ \text{sign}\,(z_1\,(t - d\,(t))) \end{array} \tag{12}$$

Due to the time delay, solutions of system (12) can switch on branches of parabola which are more and more far away from the origin (see Figure 3 with constant functions a and b). System (12) can become unstable which is proved by

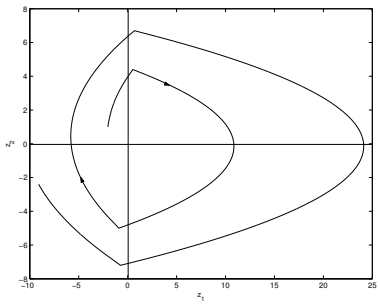

Fig. 3. Phase portrait of system (12) with $a = 1$, $b = 2$, $K = 1$, $d = 0.1$ and $T_e = 0.01$ s.

using Pontrjagin's conditions to time delay systems (see [Bhatt et al., , 1966, Case 1, Subcase 1B]). In order to ensure the stability of the system, a solution consists in modifying the control input.

For a sake of clarity, before extending the following result to system (3), consider the double integrator system (4) and the following theorem [1].

Theorem 3. Under initial conditions $(z_{1,0}, z_{2,0})$, system (4) converges to the domain

$$\mathcal{D} = \left\{ (z_1, z_2) \mid |z_1| \leq \epsilon + KT_e^2,\ |z_2| \leq 3KT_e \right\}$$

under the control input

$$u \ = \ -K\ \text{sign}(z_1 + \epsilon\ \text{sign}(z_2)) \tag{13}$$

if $K > 0$ and

$$\epsilon \ > \ T_e \sqrt{z_{2,0}^2 + 2K|z_{1,0}|} - \frac{KT_e^2}{2}. \tag{14}$$

■

Proof. Without loss of generality, suppose that, at $t = t_0$, system (4) is initialized at $(z_{1,0}, z_{2,0})$ such that $0 < \epsilon < z_{1,0} < \infty$ and $0 < z_{2,0} < \infty$. As it has been previously mentioned, the continuous function $z_1(t)$ reads as

$$z_1(t) \ = \ -K\frac{t^2}{2} + z_{2,0}t + z_{1,0}. \tag{15}$$

Then, there exists a time instant t_0 such that $z_1(t) = 0$ which reads as

$$t_0 \ = \ \frac{z_{2,0}}{K} + \sqrt{\frac{z_{2,0}^2}{K^2} + \frac{2z_{1,0}}{K}} \tag{16}$$

A sufficient condition for the convergence of system (4) to $\mathcal{D}$ is that trajectories reach a parabola closer to the origin through the commutation of the input in the z_1-interval $[0, \epsilon]$, which yields

[1] Working with sign(z_2) does not matter in an outpout feedback control scheme with a finite sampling period because, for all $t > T_e$, $z_2(t)$ may be approximated by $\frac{z_1(t) - z_1(t - Te)}{Te}$.

$$z_1(t_0 - T_e) < \epsilon$$

leading to

$$-K\frac{(t_0 - T_e)^2}{2} + z_{2,0}(t_0 - T_e) + z_{1,0} < \epsilon.$$

From the previous inequality and (16), one gets (14). It yields that there exists a time instant t_1 such that

$$|z_1(t_1)| < \epsilon,\ z_2(t_1) > 0$$

and $z_2(t_1 + T_e)$ with an opposite sign of $z_2(t_1)$. Let $z_{1,1}$ (resp. $z_{2,1}$) denote $z_{1,1} := z_1(t_1)$ (resp. $z_{2,1} := z_2(t_1)$). For a sake of clarity, suppose that $z_{2,1} > 0$ and $z_2(t_1+T_e) < 0$. Then, one gets, at $t = t_1$, (see Figure 4) [2]

$$\dot{z}_1(t_1) = z_{2,1},\ \dot{z}_2(t_1) = -K$$

It yields

$$z_2(t_1 + T_e) = z_{2,1} - KT_e < 0,$$
$$z_1(t_1 + T_e) = z_{1,1} + z_{2,1}T_e.$$

Note that one has

$$0 < z_{2,1} < KT_e.$$

Then, two cases have to be considered.

First case. Without loss of generality, suppose that

$$0 < z_1(t_1 + T_e) < \epsilon$$

Then, one gets

$$\dot{z}_1(t_1 + T_e) = z_2(t_1 + T_e),\ \dot{z}_2(t_1 + T_e) = K$$

At $t = t_1 + 2T_e$, one gets

$$z_2(t_1 + 2T_e) = z_{2,1},$$
$$z_1(t_1 + 2T_e) = z_(t_1 + T_e) + z_2(t_1 + T_e)T_e$$
$$= z_{1,1} + 2z_{2,1}T_e - KT_e^2.$$

It means that, between t_1 and $t_1 + 2T_e$, varible z_2 is keeping the same value. From previous equation, as it is not possible to establish the behavior of z_1, it is necessary to consider now two subcases (see Figure 4).

- **Point (a). Fig. 4: $\mathbf{KT_e/2 < z_{2,1} < KT_e}$.** This inequality on z_2-value at $t = t_1$ implies

  $$0 < 2z_{2,1}T_e - KT_e^2 < KT_e^2.$$

  Then, one gets

  $$z_1(t_1 + 2T_e) > z_{1,1}.$$

  This latter value of z_1 is displayed by point (c) whereas $z_1(t_1 + T_e)$ is displayed by point(b). It yields that z_1 is increasing between t_1 to t_1+2T_e, its average velocity being

  $$z_{2,1} - \frac{KT_e}{2} > 0$$

[2] In the sequel of the proof, two cases of initial conditions at $t = t_1$ are considered: point (a) is such that $KT_e/2 < z_1(t_1) < KT_e$, whereas point (d) is such that $0 < z_1(t_1) < KT_e/2$.

- **Point (d). Fig. 4: $\mathbf{KT_e/2 < z_{2,1} < KT_e}$.** This inequality on z_2-value at $t = t_1$ implies

  $$-KT_e^2 < 2z_{2,1}T_e - KT_e^2 < 0.$$

  Then, one gets

  $$z_1(t_1 + 2T_e) < z_{1,1}.$$

  This latter value of z_1 is displayed by point (f) whereas $z_1(t_1 + T_e)$ is displayed by point(e). It yields that z_1 is decreasing between t_1 and $t_1 + 2T_e$, its average velocity being

  $$z_{2,1} - \frac{KT_e}{2} < 0$$

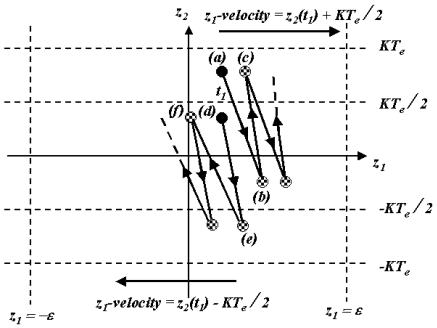

Fig. 4. Trajectories evolution in phase plan (z_1, z_2). State vector $[z_1\ z_2]^T$ at $t = t_1$ is plotted in (a) when $KT_e/2 < z_2(t_1) < KT_e$ (resp. (e) when $0 < z_2(t_1) < KT_e/2$), which induces a constant positive (resp. negative) average z_2-velocity positive.

As the average value of z_2 is constant, it implies that, in a finite time, z_1 is evolving until crossing ϵ-vertical axis. Then, the system is evolving as in the sequel described by "Second case" item.

Second case. As seen in the previous "First case", there exists a finite time instant t_2 such that

$$|z_1(t_2)| < \epsilon,\ |z_1(t_2 + T_e)| > \epsilon.$$

with $z_2(t_2 + T_e)$ with an opposite sign of $z_2(t_2)$. For a sake of clarity, but without loss of generality, suppose that (see Figure 5 - Point (A))

$$0 < z_1(t_2) < \epsilon,\quad z_1(t_2 + T_e) > \epsilon,\quad z_2(t_2) > 0.$$

From

$$\dot{z}_1(t_2) = z_2(t_2),\quad \dot{z}_2(t_2) = -K$$

and previous assumptions, it yields (Point (B) of Figure 5)

$$z_1(t_2 + T_e) > \epsilon,\ z_2(t_2 + T_e) < 0,$$

and

$$\dot{z}_1(t_2 + T_e) = z_2(t_2 + T_e),\ \dot{z}_2(t_2 + T_e) = -K.$$

As $z_1(t_2) < \epsilon$ and $z_1(t_2 + T_e) > \epsilon$, it means that

$$\epsilon - KT_e^2 < z_1(t_2) < \epsilon,\ \epsilon < z_1(t_2 + T_e) < \epsilon + KT_e^2.$$

Furthermore, one has

$$-KT_e < z_2(t_2+T_e) < 0.$$

Then, at $t = t_2 + 2T_e$, from

$$z_1(t_2+2T_e) = z_1(t_2+T_e) + z_2(t_2+T_e)T_e,$$
$$z_2(t_2+2T_e) = z_2(t_2+T_e) - KT_e,$$

one gets

$$\epsilon - KT_e^2 < z_1(t_2+2T_e) < \epsilon + KT_e^2,$$
$$-2KT_e < z_2(t_2+2T_e) < -KT_e.$$

Then, two subcases must now be considered

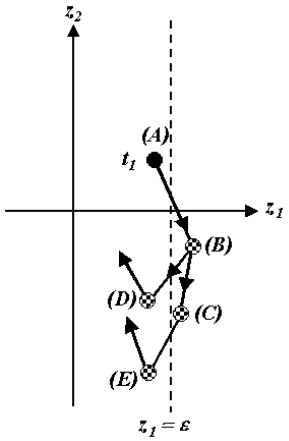

Fig. 5. Trajectories in phase plan (z_1, z_2) around ϵ-vertical axis.

- **Point (C). Fig. 5:** $\epsilon < \mathbf{z_1(t_2+2T_e)} < \epsilon + \mathbf{KT_e^2}$. One has

  $$\dot{z}_1(t_2+2T_e) = z_2,\ \dot{z}_2(t_2+2T_e) = -K$$

  At $t = t_2 + 3T_e$, one has

  $$\epsilon - 2KT_e^2 < z_1(t_2+3T_e) < \epsilon$$

  which ensures that trajectories cross ϵ-vertical axis to reach point (E) of Figure 5. Furthermore, at point (E), z_2 and dynamics of z_1 and z_2 are such that

  $$-3KT_e < z_2(t_2+3T_e) < -2KT_e$$

  and

  $$\dot{z}_1(t_2+3T_e) = z_2(t_1+3T_e), \quad \dot{z}_2(t_2+3T_e) = K$$

  Then, z_2 is encreasing while z_1 is decreasing (see arrow at point (E)).
- **Point (D). Fig. 5:** $\epsilon - \mathbf{KT_e^2} < \mathbf{z_1(t_2+T_e)} < \epsilon$. One has

  $$\dot{z}_1(t_2+2T_e) = z_2,\ \dot{z}_2(t_2+2T_e) = K$$

  At $t = t_2 + 3T_e$, one has

  $$\epsilon - 3KT_e^2 < z_1(t_2+3T_e) < \epsilon - KT_e^2$$

  which ensures that trajectories stay in the left part of (z_1, z_2) plan w.r.t. ϵ-vertical. Furthermore, z_2 and dynamics of z_1 and z_2 are such that

  $$-KT_e < z_2(t_2+3T_e) < 0$$

  and

  $$\dot{z}_1(t_2+3T_e) = z_2(t_2+3T_e),\ \dot{z}_2(t_2+3T_e) = K$$

  Then, z_2 is encreasing while z_1 is decreasing (see arrow at point (D)).

By the same way, for all initial condition $(z_{1,0}, z_{2,0})$, it can be shown that, for $K > 0$, $z_2(t)$ is evolving in $[-3KT_e\ ,\ 3KT_e]$ whereas $z_1(t)$ in $[-\epsilon - KT_e^2\ ,\ \epsilon + KT_e^2]$. ■

3.4 Extension to uncertain systems second order sliding mode control

Consider now system (3): Theorem 3 is rewritten for this class of system. Note that the convergence proof takes the same way than previously, with condition

$$K > \frac{a_M}{b_m}$$

which is the classical sliding mode gain condition ensuring that dynamics of z_2 is controlled by sign-function in spite of uncertainties.

Theorem 4. Under initial conditions $(z_{1,0}, z_{2,0})$ and assumptions H1-H3, system (3) converges to a bounded neighbourhood of the origin of the plan $(s, \dot{s})$ in a finite time under the control

$$u = -K\ \mathrm{sign}(s + \epsilon\ \mathrm{sign}(\dot{s})) \tag{17}$$

if $K > \frac{a_M}{b_m}$ and

$$\begin{aligned}
\epsilon &> \mathrm{Max}(\epsilon_1, \epsilon_2),\\
\epsilon_1 &= T_e\sqrt{z_{2,0}^2 + 2(a_M + Kb_M)|z_{1,0}|} - \frac{(a_M + Kb_M)T_e^2}{2},\\
\epsilon_2 &= T_e\sqrt{z_{2,0}^2 + 2(-a_M + Kb_m)|z_{1,0}|} - \frac{(-a_M + Kb_m)T_e^2}{2}.
\end{aligned} \tag{18}$$

■

Sketch of proof. Consider system (3) with $z_1(0) = z_{1,0} > 0$ and $z_2(0) = z_{2,0} > 0$ and u given by (17). It yields

$$\dot{z}_1(0) = z_{2,0} > 0,\ \dot{z}_2(0) = a(\cdot) - Kb(\cdot) < 0.$$

Then, one has

$$-(Kb_M + a_M)t + z_{2,0} < z_2(t) < -(Kb_m - a_M)t + z_{2,0},$$
$$z_{1m}(t) < z_1(t) < z_{1M}(t).$$

with

$$z_{1m}(t) = -(Kb_M + a_M)\frac{t^2}{2} + z_{2,0}t + z_{1,0}$$

and

$$z_{1M}(t) = -(Kb_m - a_M)\frac{t^2}{2} + z_{2,0}t + z_{1,0}.$$

Then, there exists a time t_0 such that $z_1(t_0) = 0$. It yields

$$t_{0,m} < t_0 < t_{0,M} \tag{19}$$

with

$$t_{0,m} = \frac{z_{2,0}}{Kb_M + a_M} + \sqrt{\frac{z_{2,0}^2}{(Kb_M + a_M)^2} + \frac{2z_{1,0}}{Kb_M + a_M}}$$

and

$$t_{0,M} = \frac{z_{2,0}}{Kb_m - a_M} + \sqrt{\frac{z_{2,0}^2}{(Kb_m - a_M)^2} + \frac{2z_{1,0}}{Kb_m - a_M}}$$

A sufficient condition for the convergence of system (3) is that trajectories reach a parabola closer to the origin through the commutation of the input in the z_1-interval $[0, \epsilon]$, which yields

$$z_1(t_{0,m} - T_e) < \epsilon \quad \text{and} \quad z_1(t_{0,M} - T_e) < \epsilon.$$

By replacing in the both previous inequalities $t_{0,m}$ and $t_{0,M}$ by (19), one gets (18). The end of the proof takes a similar way than the proof of Theorem 3.

4. EXAMPLE

In this section, the speed control of a series DC motor is displayed. As detailed in (Chiasson [1994]), the model of a such motor reads as

$$\begin{aligned} \dot{x}_1 &= -K_m x_1 x_2 - \frac{R_a + R_f}{K_e} x_1 + u \\ \dot{x}_2 &= -\frac{B}{J} x_2 - x_3 + \frac{K_m}{J} K x_1^2 \\ \dot{x}_3 &= 0 \end{aligned} \tag{20}$$

with x_1 the field flux, x_2 the rotor speed and x_3 the ration between load torque and inertia. R_a ($= 0.00989\ \Omega$) and R_f ($= 0.01485\ \Omega$) denote the resistance of the armature and fild windings, respectively. K_m ($= 0.004329\ Nm/Wb - A$) denotes the torque/back-emf constant, whereas B ($= .1\ T$) is the magnetic field. K_e ($= 0.057\ SI$) is a constant which lies flux and current. J is the inertia. The control objective is to drive the rotor speed to a reference value $x_{2,ref} = 1000\ rad.s^{-1}$ by using only the information of speed and the sign of acceleration: the desired trajectories have been computed by using technique displayed in Plestan et al., [2008] which ensures a finite time convergence which is *a priori* well-known. In this paper, the convergence has been stated at $t_F = 3\ s$. The controller gain value equals $K = 10^5$. Initial state variables are stated at $x_1(0) = 0.001$, $x_2(0) = 0\ rad.s^{-1}$ and $x_3(0) = 0\ N.m$, which give $\dot{x}_2(0) = 8.2183e-012\ rad.s^{-1}$. Denoting $z_1 = x_2 - x_{2,ref}$ and $z_2 = \dot{x}_2$, one gets a system as (3). From Theorem 4, with $T_e = 1\ ms$, one states $\epsilon = 0.01$. Figure 6 displays the speed rotor in case of a constant load torque on the rotor: it is shown that the motor reachs in a finite time a neighborhhod (depending on ϵ) of the objective. Figure 7 displays the speed rotor in case of dynamical perturbation load torque and thus shows the controller robustness.

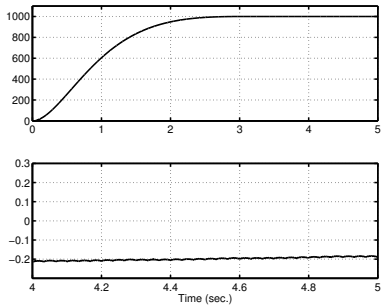

Fig. 6. **Nominal case. Top.** Rotor speed ($rad.s^{-1}$) versus time ($sec.$). **Bottom.** Rotor speed tracking error ($rad.s^{-1}$) versus time (s).

REFERENCES

G. Bartolini, A. Ferrara, E. Usai, and V.I. Utkin, *On multi-input chattering-free second-order sliding mode control*, IEEE Trans. Autom. Control, vol.45, no.9, pp.1711-1717, 2000.

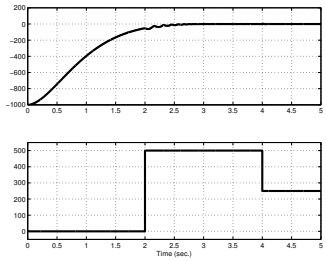

Fig. 7. **Evaluation of robustness. - Top.** Rotor speed tracking error ($rad.s^{-1}$) versus time (s). **Bottom.** Load torque (Nm) versus time (s).

S.J. Bhatt, and C.S. Hsu, *Stability criteria for second-order dynamical systems with time lag*, Journal of Applied Mechanics, vol.33, series E, no.1, pp.113-118, 1966.

J. Chiasson, *Nonlinear differential-geometric techniques for control of a series DC motor*, IEEE Trans. Control Systems Tech., vol.2, no.1, 1994.

A.F. Filippov, *Differential equations with discontinuous right-hand side*, Kluwer Academic Publishers, Dordrecht, The Netherlands, 1988.

A. Girin, F. Plestan, X. Brun, and A. Glumineau, *Position-pressure robust control of an electropneumatic actuator*, European Control Conference ECC'07, Kos, Greece, 2007.

M.K. Khan, S.K. Spurgeon, and A. Levant, *Simple output-feedback 2-sliding controller for systems of relative degree two*, European Control Conference ECC'03, Cambridge, UK, 2003.

S. Laghrouche, M. Smaoui, F. Plestan, and X. Brun, *Higher order sliding mode control based on optimal approach of an electropneumatic actuator*, International Journal of Control, vol.79, no.2, pp.119-131, 2006.

S. Laghrouche, F. Plestan, and A. Glumineau, *Higher order sliding mode control based on integral sliding surface*, Automatica, vol.43, no.3, pp.531-537, 2007.

V. Lebastard, Y. Aoustin, and F. Plestan, *Observer-based control of a walking biped robot without orientation measurement*, Robotica, vol.24, no.3, pp.385-400, 2006.

V. Lebastard, Y. Aoustin, F. Plestan, and L. Fridman, *Absolute orientation estimation based on high order sliding mode observer for a five-link walking biped robot*, 9th IEEE Workshop on Variable Structure Systems VSS'06, Alghero, Italy, 2006.

A. Levant, *Universal SISO sliding-mode controllers with finite-time convergence*, IEEE Trans. Autom. Control, vol.49, no.9, pp.1447-1451, 2001.

A. Levant, *Higher-order sliding modes, differentiation and output-feedback control*, International Journal of Control, vol.76, no.9/10, pp.924-941, 2003.

F. Plestan, A. Glumineau, and S. Laghrouche, *A new algorithm for high order sliding mode control*, International Journal of Robust and Nonlinear Control, vol.18, no.4-5, pp.441-453, 2008.

F. Plestan, A. Glumineau, and G.J. Bazani, *Position-direct current robuste control of a synchronous motor*, 46th IEEE Conference on Decision and Control CDC'07, New-orleans, Louisiana, USA, 2007.